Int. J. Solids Structures Vol. 23, No. 7, pp. 897–918, 1987
Printed in Great Britain.

0020-7683/87 $3.00+.00

DYNAMIC MODE I AND MODE II CRACK KINKING INCLUDING DELAY TIME EFFECTS

C. C. MA
Department of Mechanical Engineering, National Taiwan University, Taipei, Taiwan 107, Republic of China

and

P. BURGERS
Hibbitt, Karlsson & Sorensen, Inc., 100 Medway St., Providence, RI 02906, U.S.A.

(*Received* 6 *September* 1985; *in revised form* 4 *August* 1986)

Abstract—The dynamic stress intensity factor of an initially stationary semi-infinite crack in an unbounded linear elastic solid which kinks at some time t_f after the arrival of a stress wave is obtained as a function of crack tip velocity v_c, kink angle δ, time t and the delay time t_f. A perturbation method, using the kinking angle δ as the perturbation parameter, is used. The solutions can be compared with numerical results and other approximate results for the case of $t_f = 0$ and give excellent agreement for a large range of kinking angles. The results indicate that if a maximum energy release rate is accepted as a crack propagation criterion, then for both the incident stress wave parallel to the original crack faces and uniform dynamic loading applied to the original crack faces, the crack will propagate straight ahead of the original crack for any delay time.

INTRODUCTION

When dynamic loading is applied to a body with internal cracks, the resulting stress waves may cause the stress intensity factor at any crack tip to become equal to the value required for initiation of crack growth and continued crack propagation. The direction of propagation, as well as the velocity of crack propagation, at the instant of initiation will depend on the local stress field around the crack tip. To understand the observed bifurcation events in brittle materials, the dynamic solution for cracks which suddenly branch or kink is required. Most of the problems that have been solved involving dynamic propagation of cracks, are restricted to geometries in which the line of crack propagation is straight. Techniques have been developed to take into account time-dependent loading and arbitrary variations in crack-tip velocity for a semi-infinite crack in an infinite, isotropic, linear-elastic body. In a series of papers[1–4], Freund has essentially solved the general problem in mode I. It is only recently that experimental techniques have been developed to provide enough information about the dynamic effects in a dynamic bifurcation test for comparison with theoretical solutions. The method and results of these experiments are presented in a series of papers by Ravi-Chandar and Knauss[5–8]. With progress being made in both the analytical and experimental area, it now appears possible that there will be a good understanding of the bifurcation events in the near future.

It is only recently that correct solutions for the problem in which a crack kinks (or bifurcates) have been given. Burgers and Dempsey[9] gave some closed form results in anti-plane strain and Burgers[10] extended the range of these anti-plane results to all angles of kinking (and bifurcation) using a numerical scheme. Dempsey *et al.*[11] have used a conformal mapping technique to obtain the analytical solution for a kinking crack in mode III under stress wave loading. In plane strain, Burgers[12] and Burgers and Dempsey[13] solved the kinking and bifurcation cases numerically. An approximate method for both mode III and mixed mode I–II crack kinking under stress-wave loading was used by Achenbach *et al.*[14]. However, in all the results mentioned above, the problems have been restricted to being self-similar in the radial coordinate and time. That is, it is assumed that the new crack initiates out of the original crack tip at an angle at the same time as loading is applied to the crack faces.

To make the model more physically realistic, a finite delay time in the initiation of the non-planar crack must be included. However, if we do so, the problem loses its self-similar nature. The only solution available for this case is presented by Ma and Burgers[15] in which a perturbation method described by Kuo and Achenbach[16] is used to obtain in a simple closed form the dynamic stress intensity factor for the kinking crack under anti-plane shear loading. The error of this approximate solution of the mode III stress intensity factor with delay time $t_f = 0$ when compared to the exact values in Ref. [11] is less than 10% for any kinking angle less than 90°; if the kinking angle is less than 45°, the error is less than 2%.

The analysis undertaken here is an extension of the previous work[15] in which a crack subjected to an anti-plane strain stress wave loading was solved. In Ref. [15], the mathematics is less complicated so that the results can be obtained analytically. Also, the case of a planar stress wave which is not parallel to the original crack can be solved for, and the results indicate that for this case in mode III, if a maximum energy release rate criterion is used, the crack will still initially propagate straight ahead before kinking. The perturbation method for the plane strain case considered here is very similar to that used in the mode III case. There are principal differences in the basic mechanisms of crack branching for the anti-plane and in-plane cases. Branches of a primary crack under pure mode I (or mode II) loading generally are subjected to both mode I and mode II loading conditions whereas mixed loading conditions do not occur in anti-plane strain. Analytical results in plane strain with finite delay time are so far limited to the case when no kinking occurs[2–4].

We consider the dynamic crack growth out of the original semi-infinite crack at an angle to the original crack at some time after the longitudinal (or transverse) stress wave loading initially interacts with the crack tip. A perturbation method is used to obtain the first-order solution near the kinking crack tip. By setting the finite delay time t_f to zero, this solution agrees closely with the results in Ref. [14] up to the kinking angle of about 70°. We find the solutions of the mode I stress intensity factor have the same accuracy as found in the mode III case. The mode II stress intensity factor is also within 13% error if compared to numerical results[12]. This good agreement suggests that the wedge geometry of the kinked crack has only a minor effect on the dynamic stress intensity factor. When the kinking angle δ is zero, the new crack will propagate straight along the original crack path, and the solution will reduce to the exact solution shown in Ref. [3]. The energy flux into the propagating kinked crack tip can be obtained from the dynamic stress intensity factors, and these results are discussed in terms of an assumed fracture criterion.

DESCRIPTION OF PROBLEMS

We consider a stationary, semi-infinite, straight crack in an initially stress-free, isotropic linear-elastic full space. The sharp crack, which will be referred to as the original crack, lies along the negative x-axis with the origin of the coordinate system at the crack tip. The incident longitudinal wave (or transverse wave) strikes the stationary crack tip at time $t = 0$. A short time later, at $t = t_f$, a crack referred to as the new crack, propagates out of the tip of the semi-infinite crack with a constant velocity v_c (less than the Rayleigh wave speed) making an angle δ with the original crack. The geometry for the kinked crack under consideration with the wavefront pattern for planar normal stress wave loading is shown in Fig. 1.

The field solution for a kinked crack geometry can be considered as the superposition of the field generated by diffraction of the incident wave by the stationary crack and the field from the new crack faces subjected to crack-face tractions which are opposite in sign to the stresses computed from the stationary crack problem. For in-plane problems, the fields generated by kinking of a semi-infinite crack upon diffraction of a longitudinal or transverse stress wave are extremely difficult to analyze. It involves coupled integral equations, which must be solved numerically, see Refs [12, 13].

For the anti-plane case, it was shown that the first-order approximation of the dynamic stress intensity factor for a kinked crack can be expressed by the stress intensity factor for

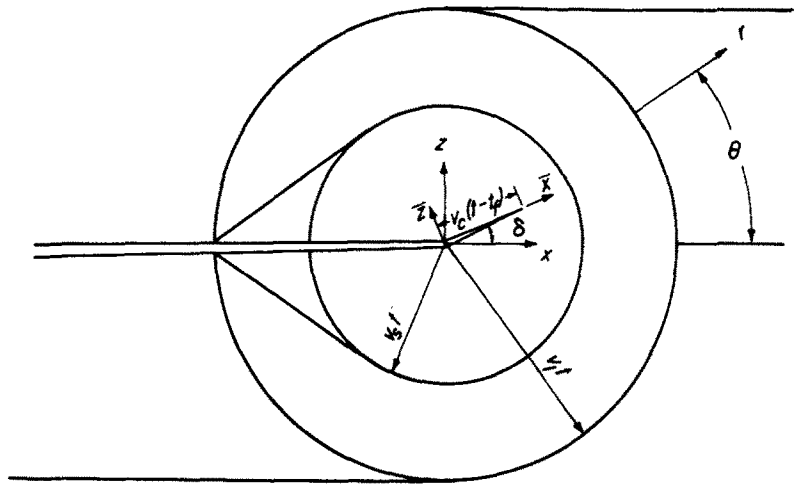

Fig. 1. Stress wavefront pattern for a planar stress wave impacting a kinking crack.

a straight crack, propagating in its own plane, subjected to the negative of the traction computed from the stationary crack problem along the line of the kinked crack. We follow the same approach here for the in-plane problems. The procedures to construct the final solution are similar to the anti-plane problem which was solved by Ma and Burgers[15]. In the next section, some fundamental solutions needed for solving the dynamic stress intensity factor of a kinking crack are presented.

REQUIRED FUNDAMENTAL SOLUTIONS

A homogeneous, isotropic linearly elastic medium is governed by the two-dimensional wave equations

$$\nabla^2\phi - a^2\ddot{\phi} = 0 \tag{1}$$

$$\nabla^2\psi - b^2\ddot{\psi} = 0 \tag{2}$$

where

$$a = \sqrt{\left(\frac{\rho}{\lambda+2\mu}\right)} = \frac{1}{v_l}, \qquad b = \sqrt{\left(\frac{\rho}{\mu}\right)} = \frac{1}{v_s}.$$

Equations (1) and (2) are the uncoupled wave equations. Because of their associated modes of deformation, ϕ and ψ are referred to as the longitudinal and shear wave potentials, a and b are the slowness of longitudinal and shear waves, respectively, μ and ρ are the shear modulus and the mass density of the material, and λ is the Lame elastic constant.

Normal and shear loading applied on the stationary crack

For the normal step loading applied uniformly on the crack faces, the deformation will occur in mode I. The following mixed boundary conditions on $z = 0$ are considered:

$$\sigma^{\mathrm{I}}_{zz}(x,0,t) = -\sigma_0 H(t) \qquad \text{for} \qquad -\infty < x < 0 \tag{3a}$$

$$\sigma^{\mathrm{I}}_{xz}(x,0,t) = 0 \qquad \text{for} \qquad -\infty < x < \infty \tag{3b}$$

$$w(x,0,t) = 0 \qquad \text{for} \qquad 0 < x < \infty. \tag{3c}$$

Here w is the component of displacement in the z-direction, and H represents the unit step function. The definition of the problem is completed by specifying zero initial conditions

and by requiring the solution to satisfy the equations governing the motion of an elastic solid. The details of the plane strain problem of diffraction of a pulse by a stationary crack have been presented by De Hoop[17], and only the pertinent results of the full field solutions for stresses $\theta < \pi/2$ are presented

$$\frac{\sigma^1_{zz}}{A} = \int_{ar}^{t} \mathrm{Im}\left[\frac{(2\lambda^2-b^2)^2\Phi(s)}{\lambda(a+\lambda)^{1/2}}\right]_{\lambda=\lambda_L} \mathrm{d}s + \int_{br}^{t} \mathrm{Im}\,[4\lambda(a-\lambda)^{1/2}(b^2-\lambda^2)^{1/2}\Phi(s)]_{\lambda=\lambda_T}\,\mathrm{d}s \quad (4a)$$

$$\frac{\sigma^1_{xz}}{A} = \int_{ar}^{t} \mathrm{Im}\,[2(2\lambda^2-b^2)\,(a-\lambda)^{1/2}\Phi(s)]_{\lambda=\lambda_L}\,\mathrm{d}s - \int_{br}^{t} \mathrm{Im}\,[2(2\lambda^2-b^2)\,(a-\lambda)^{1/2}\Phi(s)]_{\lambda=\lambda_T}\,\mathrm{d}s \quad (4b)$$

$$\frac{\sigma^1_{xx}}{A} = -\int_{ar}^{t} \mathrm{Im}\left[\frac{(2\lambda^2-b^2)\,(2\lambda^2+b^2-2a^2)\Phi(s)}{\lambda(a+\lambda)^{1/2}}\right]_{\lambda=\lambda_L}\mathrm{d}s - \int_{br}^{t} \mathrm{Im}\,[4\lambda(a-\lambda)^{1/2}(b^2-\lambda^2)^{1/2}\Phi(s)]_{\lambda=\lambda_T}\,\mathrm{d}s \quad (4c)$$

where

$$A = \frac{\sqrt{a}\,\sigma_0}{\pi c k S^0_+(0)}, \qquad k = 2(b^2-a^2),$$

$$\lambda_L(s) = -\frac{s}{r}\cos\theta + \mathrm{i}\left(\frac{s^2}{r^2}-a^2\right)^{1/2}\sin\theta \quad (5a)$$

$$\lambda_T(s) = -\frac{s}{r}\cos\theta + \mathrm{i}\left(\frac{s^2}{r^2}-b^2\right)^{1/2}\sin\theta \quad (5b)$$

$$S^0_{\pm}(\lambda) = \exp\left(-\frac{1}{\pi}\int_a^b \tan^{-1}\left[\frac{4y^2(y^2-a^2)^{1/2}(b^2-y^2)^{1/2}}{(b^2-2y^2)^2}\right]\frac{\mathrm{d}y}{y\pm\lambda}\right), \quad (6)$$

$$\Phi(s) = \frac{\partial\lambda/\partial s}{(\lambda-c)S^0_-(\lambda)}$$

$c = 1/v_r$ is the slowness of Rayleigh wave of the material and satisfies the equation

$$(2c^2-b^2)^2 + 4c^2(a^2-c^2)^{1/2}(b^2-c^2)^{1/2} = 0.$$

As mentioned in Ref. [15], the second term which is $O(1)$ in the asymptotic expansion as $r \to 0$ in eqns (4) will play a significant role in the crack kinking problem. The complete result for the second term of this expansion has not yet appeared in the dynamic fracture literature, to the best of our knowledge. By changing the integration on the real axis to the complex plane and using the residue theorem, the results for the second term as $r \to 0$ can be obtained by evaluating the contributions from the poles. As $r \to 0$, the first two terms for the stresses are

$$\sigma_{zz}^{I} \approx \frac{2}{\pi}\sigma_0 w_0 \left(\frac{t}{r}\right)^{1/2} \cos\frac{\theta}{2}\left[1+\sin\frac{\theta}{2}\sin\frac{3\theta}{2}\right]-\sigma_0+o(1) \tag{7a}$$

$$\sigma_{xz}^{I} \approx \frac{2}{\pi}\sigma_0 w_0 \left(\frac{t}{r}\right)^{1/2} \cos\frac{\theta}{2}\sin\frac{\theta}{2}\cos\frac{3\theta}{2}+o(1) \tag{7b}$$

$$\sigma_{xx}^{I} \approx \frac{2}{\pi}\sigma_0 w_0 \left(\frac{t}{r}\right)^{1/2} \cos\frac{\theta}{2}\left[1-\sin\frac{\theta}{2}\sin\frac{3\theta}{2}\right]-\sigma_0 C_{xx}+o(1) \tag{7c}$$

where

$$w_0 = \frac{\sqrt{a}}{cS_+^0} = \frac{\sqrt{(2a(b^2-a^2))}}{b^2},$$

$$C_{xx} = \frac{b^2-2a^2}{b^2} + \frac{\sqrt{a}\,(2c^2-b^2)}{c^2 S_+^0(0) S_-^0(c)\,(a+c)}.$$

The first term shows the square root singularity as $r \to 0$; the angular dependence is the same as the static solution. The second term is a constant and depends only on the magnitude of the loading σ_0 and the material properties.

For the shear step loading applied uniformly on the crack faces, the deformation will occur in mode II. The boundary conditions are then

$$\sigma_{zz}^{II}(x,0,t) = 0 \qquad \text{for} \qquad -\infty < x < \infty \tag{8a}$$

$$\sigma_{xz}^{II}(x,0,t) = -\sigma_0 H(t) \qquad \text{for} \qquad -\infty < x < 0 \tag{8b}$$

$$u^*(x,0,t) = 0 \qquad \text{for} \qquad 0 < x < \infty \tag{8c}$$

where u^* is the component of displacement in the x-direction. The full field solutions for stresses evaluated for $\theta < \pi/2$ are

$$\frac{\sigma_{zz}^{II}}{B} = -\int_{ar}^{t} \operatorname{Im}\left[2(b^2-2\lambda^2)(b-\lambda)^{1/2}\Phi(s)\right]_{\lambda=\lambda_L} ds + \int_{br}^{t} \operatorname{Im}\left[2(b^2-2\lambda^2)(b-\lambda)^{1/2}\Phi(s)\right]_{\lambda=\lambda_T} ds \tag{9a}$$

$$\frac{\sigma_{xz}^{II}}{B} = \int_{ar}^{t} \operatorname{Im}\left[4\lambda(b-\lambda)^{1/2}(a^2-\lambda^2)^{1/2}\Phi(s)\right]_{\lambda=\lambda_L} ds + \int_{br}^{t} \operatorname{Im}\left[\frac{(2\lambda^2-b^2)^2\Phi(s)}{\lambda(b+\lambda)^{1/2}}\right]_{\lambda=\lambda_T} ds \tag{9b}$$

$$\frac{\sigma_{xx}^{II}}{B} = -\int_{ar}^{t} \operatorname{Im}\left[2(b-\lambda)^{1/2}(2\lambda^2+b^2-2a^2)\Phi(s)\right]_{\lambda=\lambda_L} ds - \int_{br}^{t} \operatorname{Im}\left[2(b-\lambda)^{1/2}(b^2-2\lambda^2)\Phi(s)\right]_{\lambda=\lambda_T} ds \tag{9c}$$

where

$$B = \frac{\sqrt{b}\,\sigma_0}{\pi c k S_+^0(0)}.$$

For $r \to 0$, the leading two terms of the asymptotic expansion of eqns (9) are

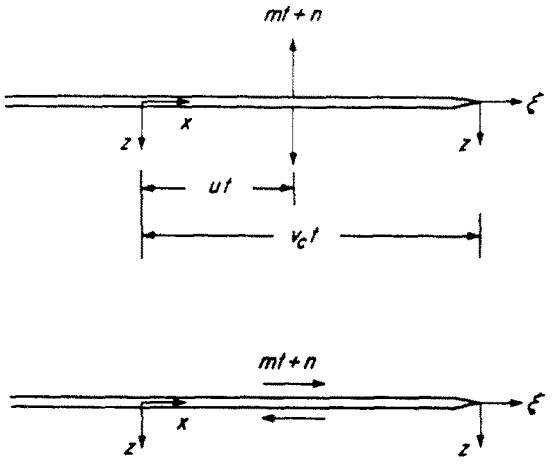

Fig. 2. Normal and shear point loads propagating out with velocity u along the faces of the semi-infinite crack, growing with speed v_c.

$$\sigma_{zz}^{II} \approx \frac{2}{\pi}\sigma_0 u_0 \left(\frac{t}{r}\right)^{1/2} \cos\frac{\theta}{2}\sin\frac{\theta}{2}\cos\frac{3\theta}{2} + o(1) \tag{10a}$$

$$\sigma_{xz}^{II} \approx \frac{2}{\pi}\sigma_0 u_0 \left(\frac{t}{r}\right)^{1/2} \cos\frac{\theta}{2}\left[1-\sin\frac{\theta}{2}\sin\frac{3\theta}{2}\right] - \sigma_0 + o(1) \tag{10b}$$

$$\sigma_{xx}^{II} \approx -\frac{2}{\pi}\sigma_0 u_0 \left(\frac{t}{r}\right)^{1/2} \sin\frac{\theta}{2}\left[2+\cos\frac{\theta}{2}\cos\frac{3\theta}{2}\right] + o(1) \tag{10c}$$

where

$$u_0 = \frac{\sqrt{b}}{cS_+^0(0)} = \frac{\sqrt{(2b(b^2-a^2))}}{b^2}.$$

Normal and shear point loads varying linearly in time for a growing crack

The method of solution follows that described by Freund[1–4] and uses the superposition of forces applied to the newly growing crack faces, to cancel out the stresses obtained along the new crack line due to the normal and shear stress wave loading on the stationary crack. This requires the solution for normal and shear point loads, which grow linearly with time and propagate out from the origin along the new crack at constant velocity u as the crack starts to propagate. Suppose that the crack tip is at rest at $x = 0$ and there are no loads acting on the body for $t < 0$. At time $t = 0$, the crack tip begins to move in the x-direction at speed v_c and simultaneously a symmetric pair of concentrated normal forces appears at the crack tip, tending to open the crack. For $t > 0$, the concentrated forces begin to move in the x-direction with speed $u < v_c$, as shown in Fig. 2. The magnitude of the forces increases linearly in time. The boundary conditions are

$$\begin{aligned}
(\sigma_{zz}^F)_1(x,0,t) &= (mt+n)\Delta(x-ut)H(t) \qquad \text{for} \qquad -\infty < x < v_c t \\
(\sigma_{xz}^F)_1(x,0,t) &= 0 \qquad \text{for} \qquad -\infty < x < \infty \\
w(x,0,t) &= 0 \qquad \text{for} \qquad v_c t < x < \infty
\end{aligned} \tag{11}$$

where Δ is the Dirac delta function, m and n are arbitrary parameters which are independent of x and t. The x-coordinate is eliminated in favor of a new coordinate $\xi = x - v_c t$. The exact solution of this problem can be obtained by means of Laplace transform methods and

the Wiener–Hopf technique. The normal stress on the plane $z = 0$ ahead of the crack tip is given in Ref. [3] as

$$(\sigma_{zz}^F)_1(\xi,0,t) = \frac{1}{2\pi i}\int_{B_1}\frac{1}{2\pi i}\int_{B_2}\left(\left[\frac{mh^2}{sw_+(\lambda)}\right]\left[\frac{w_+(h)}{(\lambda-h)}\right]_h - \left[\frac{nhw_+(h)}{(\lambda-h)w_+(\lambda)}\right]\right)e^{s(t+\lambda\xi)}\,d\lambda\,ds \tag{12}$$

where

$$S_\pm(\lambda) = \exp\left(-\frac{1}{\pi}\int_{a_{2,1}}^{b_{2,1}}\tan^{-1}\left[\frac{4\eta^2|\alpha|\,|\beta|}{2\eta^2-b^2-b^2\eta^2/d^2\mp 2b^2\eta/d)^2}\right]\frac{d\eta}{\eta\pm\lambda}\right) \tag{13}$$

$$\alpha(\lambda) = (a^2-\lambda^2+a^2\lambda^2/d^2-2a^2\lambda/d)^{1/2}$$

$$\beta(\lambda) = (b^2-\lambda^2+b^2\lambda^2/d^2-2b^2\lambda/d)^{1/2}$$

$$\alpha_\pm = [a\pm\lambda(1\mp a/d)]^{1/2}$$

$$w_+(\lambda) = \frac{\alpha_+(\lambda)}{(\lambda+c_2)S_+(\lambda)}$$

$$a_2 = \frac{a}{1-a/d}, \qquad b_2 = \frac{b}{1-b/d}, \quad c_2 = \frac{c}{1-c/d}.$$

The slowness of the crack velocity is $d = 1/v_c$; B_1 and B_2 are the usual inversion paths for one and two-sided Laplace transforms. The parameter $h = 1(v_c-u)$ is the inverse of the relative speed between the moving load and the crack-tip, and subscript h denotes differentiation with respect to h. The stress intensity factor for the solution may be extracted by examining the behaviour of eqn (12) as $\xi \to 0^+$, with the result

$$K_I^F = \lim_{\xi\to 0^+}(\sqrt{(2\pi\xi)}\,(\sigma_{zz}^F)_1) = \frac{2mh^2w_+'\sqrt{(2t)}}{\sqrt{\pi}(1-a/d)^{1/2}} - \frac{\sqrt{2}\,nhw_+(h)}{(1-a/d)^{1/2}\sqrt{(\pi t)}} \tag{14}$$

where

$$w_+' = \frac{\partial w_+(h)}{\partial h}.$$

The other fundamental solution needed is very similar to eqns (11). Instead of applying concentrated normal forces, we have concentrated shear forces appearing at the crack tip and moving in the x-direction with speed u. The boundary conditions become

$$\begin{aligned}
&(\sigma_{zz}^F)_2(x,0,t) = 0 \qquad \text{for} \qquad -\infty < x < \infty \\
&(\sigma_{xz}^F)_2(x,0,t) = (mt+n)\Delta(x-ut)H(t) \qquad \text{for} \qquad -\infty < x < u_c t \\
&u^*(x,0,t) = 0 \qquad \text{for} \qquad v_c t < x < \infty.
\end{aligned} \tag{15}$$

Following the same analysis as Ref. [3], we find the stress intensity factor for this case is

$$K_{II}^{F} = \lim_{\xi \to 0^+} (\sqrt{(2\pi\xi)}\,(\sigma_{zz}^{F})_2) = \frac{2mh^2 u'_+ \sqrt{(2t)}}{\sqrt{\pi}\,(1-b/d)^{1/2}} - \frac{\sqrt{2}\,nhu_+(h)}{(1-b/d)^{1/2}\sqrt{(\pi t)}} \tag{16}$$

where

$$u_+(h) = \frac{\beta_+(h)}{(h+c_2)S_+(h)}$$

$$\beta_\mp(h) = [b \pm h(1 \mp b/d)]^{1/2}.$$

This result first appeared in Ref. [18].

MIXED MODE CRACK KINKING DUE TO AN INCIDENT LONGITUDINAL WAVE

We consider the incident longitudinal stress wave of the form

$$\sigma_{zz}^{i} = \sigma_0 H(tv_1 - z). \tag{17}$$

The stresses of the stationary crack problem in the polar coordinate are

$$\sigma_{\theta\theta}^{s} = \sigma_{\theta\theta}^{i} + \sigma_{\theta\theta}^{d}, \qquad \sigma_{\theta r}^{s} = \sigma_{\theta r}^{i} + \sigma_{\theta r}^{d} \tag{18a,b}$$

where

$$\sigma_{\theta\theta}^{i} = \sigma_0\left[1 - 2\left(\frac{a}{b}\right)^2 \sin^2\theta\right] \tag{19a}$$

$$\sigma_{\theta r}^{i} = \sigma_0\left(\frac{a}{b}\right)^2 \sin 2\theta \tag{19b}$$

$$\sigma_{\theta\theta}^{d} = \frac{1}{2}(1-\cos 2\theta)\sigma_{xx}^{I} + \frac{1}{2}(1+\cos 2\theta)\sigma_{zz}^{I} - \sin 2\theta\,\sigma_{xz}^{I} \tag{20a}$$

$$\sigma_{\theta r}^{d} = -\frac{1}{2}\sin 2\theta\,\sigma_{xx}^{I} + \frac{1}{2}\sin 2\theta\,\sigma_{zz}^{I} + \cos 2\theta\,\sigma_{xz}^{I} \tag{20b}$$

where σ_{xx}^{I}, σ_{xz}^{I} and σ_{zz}^{I} are given in eqns (4). The first-order approximation of the dynamic stress intensity factor for a kinked crack with delay time t_f can be expressed by the stress intensity factor for a straight crack propagating in its own plane subjected to the negative of the traction given in eqns (18) on the crack faces. This approximation is discussed more fully in Ref. [15]. The boundary condition becomes:

(1) for the mode I stress intensity factor

$$\sigma_{zz} = 0 \qquad \text{for} \qquad \bar{x} < 0 \tag{21a}$$

$$\sigma_{zz} = \sigma_{\theta\theta}^{s}(\bar{x}/t, \theta = \delta) \qquad \text{for} \qquad 0 < \bar{x} < v_c(t - t_f); \tag{21b}$$

(2) for the mode II stress intensity factor

$$\sigma_{zx} = 0 \qquad \text{for} \qquad \bar{x} < 0 \tag{22a}$$

$$\sigma_{zx} = -\sigma_{\theta r}^{s}(\bar{x}/t, \theta = \delta) \qquad \text{for} \qquad 0 < \bar{x} < v_c(t - t_f) \tag{22b}$$

where the $\bar{x}$-axis lies along the kinked crack line and δ is the kinked angle as shown in Fig. 1.

Mode I stress intensity factor

Using the superposition scheme described in Ref. [3], the stress intensity factor due to the loading from the diffraction part of the stationary crack field (i.e. $-\sigma_{\theta\theta}^{d}$) in eqns (21), can be constructed by choosing $m = -1$, $n = -t^* = -ht_f/d$, and replacing t by $t-t^*$ in eqn (14) and integrating over the appropriate range of $u = \bar{x}/t$. The mode I stress intensity factor for the propagating kinked crack duc to this loading is

$$\begin{aligned} K_I^L(t, v_c, \delta) &= \int_0^{v_c(t-t_f)/t} K_I^F(m=-1, n=-t^*, t-t^*)\sigma_{\theta\theta}^{d}\left(\frac{1}{u}, \delta\right) \mathrm{d}u \\ &= -\int_d^{d^*} 2\left[\frac{2t_f}{\pi d(1-a/d)}\right]^{1/2} [w_+(h)(d^*-h)^{1/2}]_h \sigma_{\theta\theta}^{d}\left(\frac{h}{v_c h-1}, \delta\right) \mathrm{d}h \end{aligned} \tag{23}$$

where

$$d^* = \frac{t}{v_c t_f}.$$

The integral in eqn (23) is suited to integration by parts. The advantage of this is that it reduces one order of integration which saves computation time. It also gives a more tractable form than eqn (23), allowing us to get very simple closed form results in some special cases. By careful analysis, we find that the function $\sigma_{\theta\theta}^{d}$ has a square root singularity at $h = d$. Hence, if integration by parts is applied, neither the integrated term nor the remaining integral will exist, even though the sum exists. To get around this difficulty, the method given in Ref. [3] as applied in Ref. [15] is needed. The lower limit of integration in eqn (23) is replaced by $d+\varepsilon$, where $\varepsilon \ll d$. It can be shown that those terms which are singular at $\varepsilon = 0$ exactly cancel each other and the desired result can be obtained by taking the limit as $\varepsilon \to 0$.

Integration by parts of eqn (23) and making use of the explicit expression for $\sigma_{\theta\theta}^{d}$ in eqns (20) and (4a)–(4c) yields

$$\begin{aligned} (K_I^L)_d(t, v_c, \delta) = \lim_{\varepsilon \to 0} 2\sigma_0 \left[\frac{2t_f}{\pi d(1-a/d)}\right]^{1/2} \Bigg\{ & w_+(d)(d^*-d)^{1/2} \\ & \times \left[\frac{2}{\pi}\frac{dw_0}{\varepsilon^{1/2}}\cos^3\frac{\delta}{2} - \cos^2\delta - C_{xx}\sin^2\delta\right] \\ & + \int_{d+\varepsilon}^{d^*} w_+(h)(d^*-h)^{1/2}(\sigma_{\theta\theta}^{d})_h \,\mathrm{d}h \Bigg\} + o(1). \end{aligned} \tag{24}$$

It is convenient to rewrite ε in the following manner

$$\frac{1}{\varepsilon^{1/2}} = \frac{1}{2(d^*-d)^{1/2}}\left[\int_{d+\varepsilon}^{d^*} \frac{(d^*-h)^{1/2}}{(h-d)^{3/2}} + \pi\right].$$

Then, eqn (24) becomes

$$(K_I^L)_d(t, v_c, \delta) = 2\sigma_0\left[\frac{2t_f}{\pi d(1-a/d)}\right]^{1/2}\left\{-w_+(d)(d^*-d)^{1/2}\right.$$

$$\times[\cos^2\delta + C_{xx}\sin^2\delta] + \omega_0 d w_+(d)\cos^3\frac{\delta}{2} + \frac{\omega_0 d}{\pi}\int_d^{d^*}\frac{(d^*-h)^{1/2}}{(h-d)^{1/2}}$$

$$\left.\times\left[\frac{w_+(d)}{(h-d)}\cos^3\frac{\delta}{2} - \frac{w_+(h)d^{5/2}}{k(h-d)^3}(\sigma_{\theta\theta}^L)_h^*\right]\mathrm{d}h\right\} + o(1). \quad (25)$$

The complete form of $(\sigma_{\theta\theta}^L)_h^*$ is shown in Appendix A. The integral in eqn (25) seems to have a very strong singularity up to power 7/2 in the lower limit, but actually, $(\sigma_{\theta\theta}^L)_h^*$ is of $O(\varepsilon^2)$ as $\varepsilon = h-d \to 0$, and

$$\frac{w_+(d)}{(h-d)}\cos^3\frac{\delta}{2} - \frac{w_+(h)d^{5/2}}{k(h-d)^3}(\sigma_{\theta\theta}^L)_h^* = O(1) \qquad \text{as } \varepsilon \to 0.$$

Hence, the integral in eqn (25) contains only a square root singularity at the lower limit and goes to zero as the square root in the upper limit. This term is then suitable for numerical integration using a suitable Jacobi–Gaussian type quadrature.

The solution in eqn (25) is due to the diffracted field, eqn (20), only. The stress intensity factor due to the incident field, eqn (19), can be easily obtained as follows:

$$(K_I^L)_i(t, v_c, \delta) = \int_0^{v_c(t-t_f)} K_I^F\left(m=0, n=-1, t-t_f-\frac{x_0}{v_c}\right)\sigma_{\theta\theta}^i\,\mathrm{d}x_0$$

$$= \frac{2\sqrt{2}\,\sigma_0 t_f^{1/2} w_+(d)(d^*-d)^{1/2}}{\sqrt{\pi}(1-a/d)^{1/2}d^{1/2}}\left[1-2\left(\frac{a}{b}\right)^2\sin^2\delta\right]. \quad (26)$$

Hence, the first-order approximation of the mode I stress intensity factor for the kinking crack due to the normal loading on the original crack faces is expressed in eqn (25) and the solution for the stress wave loading is the sum of the contributions due to diffracted and incident fields given in eqns (25) and (26)

$$K_I^L = (K_I^L)_d + (K_I^L)_i. \quad (27)$$

Some special cases can simplify the complicated integral that appears in eqn (25) to give simple closed form results for eqn (27). This can then be used as a check for the numerical calculation of the general cases. For the kinking angle $\delta = 0$, the crack propagates straight out of the original crack and eqn (27) will reduce to the solution derived by Freund[3]

$$K_I^L = 2\sqrt{\left(\frac{2t}{\pi}\right)}\sigma_0 w_0 \kappa(d) = K_I^s \kappa(d) \qquad \text{for} \qquad \delta = 0 \quad (28)$$

where

$$\kappa(d) = \frac{d}{S_+(d)(d+c_2)(1-a/d)^{1/2}}.$$

The function $\kappa(d)$ depends only on the crack speed $v_c = 1/d$ and material properties. The value of $\kappa(d)$ decreases from unity at $v_c = 0$ to zero when the crack speed reaches the Rayleigh wave speed. $\kappa(d)$ is a universal function of the instantaneous crack tip speed and K_I^s is the stress intensity factor for a stationary crack under the same time-dependent loading. It is worth noting that the solution in eqn (28) is an exact result, without any

approximation made in this case. Referring to eqn (28), the interesting result is that the stress intensity factor is independent of the delay time t_f for stress wave loading. In general, however, the stress intensity factor for the kinking crack does depend on the delay time as shown in eqns (25) and (27).

It is clear that the most significant time scale involved should be in the region when the crack kinking has just occurred. The field quantities change very rapidly at this time period and it certainly plays an important role in the crack kinking events. The instant of initiation of the kinked crack is at time $t = t_f + \varepsilon$, $\varepsilon \to 0$. For this special case, we have

$$\begin{aligned} K_I^L &= 2\sqrt{\left(\frac{2}{\pi}\right)}\sigma_0 w_0 \kappa(d) t^{1/2} \cos^3 \frac{\delta}{2} \\ &= K_I^s \kappa(d) \cos^3 \frac{\delta}{2} \qquad \text{as } t \to t_f. \end{aligned} \tag{29}$$

That is, the stress intensity factor just after the initiation of the kinked crack, given in eqn (29), has the form of the universal function of the crack-tip speed $\kappa(d)$ times the stress intensity factor appropriate for the given diffraction process but with no crack-tip motion times the spatial angular dependence of the stationary crack field.

Mode II stress intensity factor

The mode II stress intensity factor of the kinking crack subjected to a longitudinal stress wave can be obtained from the boundary condition shown in eqn (22). Following a similar analysis as in the mode I case, the mode II stress intensity factor due to the diffracted field, eqn (20), can be expressed as

$$\begin{aligned} (K_{II}^L)_d(t, v_c, \delta) &= \int_0^{v_c(t-t_f)/t} K_{II}^F(m=-1, n=-t^*, t-t^*)\sigma_{\theta r}^d\left(\frac{1}{u}, \delta\right) du \\ &= 2\sigma_0\left[\frac{2t_f}{\pi d(1-b/d)}\right]^{1/2}\left\{-u_+(d)(d^*-d)^{1/2}\frac{1-C_{xx}}{2}\sin 2\delta\right. \\ &\quad + \frac{w_0 du_+(d)}{4}\left(\sin\frac{\delta}{2}+\sin\frac{3\delta}{2}\right) + \frac{w_0 d}{\pi}\int_d^{d^*}\frac{(d^*-h)^{1/2}}{(h-d)^{1/2}}\left[\frac{u_+(d)}{4(h-d)}\right. \\ &\quad \left.\left.\times\left(\sin\frac{\delta}{2}+\sin\frac{3\delta}{2}\right) - \frac{u_+(h)d^{5/2}}{k(h-d)^3}(\sigma_{\theta r}^L)_h^*\right] dh\right\} + o(1). \end{aligned} \tag{30}$$

Details of $(\sigma_{\theta r}^L)_h^*$ are given in Appendix A. The mode II stress intensity factor due to the incident field, eqn (19b), is

$$\begin{aligned} (K_{II}^L)_i(t, v_c, \delta) &= \int_0^{v_c(t-t_f)} K_{II}^F\left(m=0, n=-1, t-t_f-\frac{x_0}{v_c}\right)\sigma_{\theta r}^i\, dx_0 \\ &= \frac{2\sqrt{2}\,\sigma_0 t_f^{1/2} u_+(d)(d^*-d)^{1/2}}{\sqrt{\pi}(1-b/d)^{1/2}d^{1/2}}\left(\frac{a}{b}\right)^2 \sin 2\delta. \end{aligned} \tag{31}$$

Hence

$$K_{II}^L = (K_{II}^L)_d + (K_{II}^L)_i \tag{32}$$

and immediately after the crack kinks

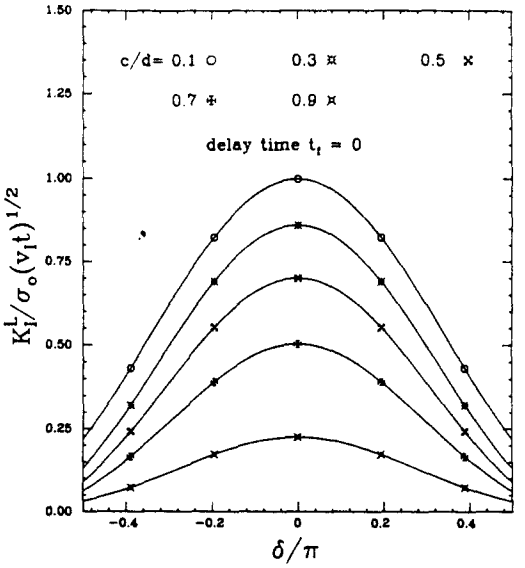

Fig. 3.The normalized mode I stress intensity factor vs kinking angle for $t_f = 0$ for different values of crack speed due to incident longitudinal stress wave loading.

$$K_{II}^L = \frac{\sqrt{2}\,\sigma_0 w_0 u_+(d)\,(dt)^{1/2}}{2\sqrt{\pi}\,(1-b/d)^{1/2}}\left(\sin\frac{\delta}{2}+\sin\frac{3\delta}{2}\right) \qquad \text{as } t\to t_f. \tag{33}$$

Energy fluxes into the kinking crack tip

For mixed mode I–II fracture, the energy flux into the propagating crack tip can be written (see Ref. [19] for a general derivation and Ref. [14] for an application) in terms of the corresponding dynamic stress intensity factors

$$\begin{aligned} E &= -\frac{b^2}{2\mu d^3 R(d)}\left[\left(1-\frac{a^2}{d^2}\right)^{1/2}(K_I)^2+\left(1-\frac{b^2}{d^2}\right)^{1/2}(K_{II})^2\right] \\ &= \frac{\sigma_0^2 t}{2\mu b^2}E^* \end{aligned} \tag{34}$$

where

$$R(d) = \left(\frac{b^2}{d^2}-2\right)^2 - 4\left(1-\frac{a^2}{d^2}\right)^{1/2}\left(1-\frac{b^2}{d^2}\right)^{1/2}.$$

In the following calculations of E^*, the stress intensity factor might show a negative value. A negative mode I stress intensity factor would correspond to the contact of the crack faces near the crack tip and in this case, K_I is set identically equal to zero. Under the smooth frictionless crack faces assumption, the effect on the negative mode II stress intensity factor may be ignored.

Numerical results

In order to compare the calculations with other available results[12, 14], we examine the special case of no finite delay time; that is the crack kinks at the instant the incident stress wave strikes the original crack tip. Figures 3 and 4 show the dimensionless mode I and mode II stress intensity factor for various values of the crack kinking angle δ and normalized crack tip speed v_c/v_r by an incident longitudinal stress wave loading. Note that for all calculations in this paper, a Poisson's ratio of 1/4 is used which gives a ratio of wave speed $v_l = \sqrt{3}\,v_s$, $v_r = 1.884v_l$. The results are nearly the same up to $\delta = 70°$ when compared to the calculations in Ref. [14] which also uses the same approximate method. In the range

$\delta = 70$–$90°$, the above results show a smooth continuous decrease, which agree more closely with the numerical results in Ref. [12], than the results presented in Ref. [14].

The first-order accurate method used in this paper shows quite satisfactory agreement with Ref. [12] for $t_f = 0$. For kinking angles less than 45°, the error introduced by using this approximate method is within 2% for the mode I stress intensity factor and within 5% for the mode II stress intensity factor when compared with the results in Ref. [12]. Even for the high kinking angles, for δ near 90°, the error is within 8% for mode I and within 13% for mode II. The accuracy of the approximate method for the in-plane kinking problem is similar to that in the anti-plane case[15]. The better agreement for the mode I stress intensity factor than the mode II can be explained by Fig. 5 shown in Ref. [12]. It shows the stress intensity factor obtained applying a constant normal (or shear) traction to the newly kinked crack faces. The results show that the mode I case has a flatter curve than mode II in the whole kinking range. This implies that for finite loads on the new crack faces, the geometry of the corner has less effect on the mode I stress intensity factor at the kinked crack tip. The effect of the corner geometry on the whole kinking range will be at most 8% for the mode I stress intensity factor and 15% for mode II. These results are consistent with the accuracy we get by using the approximate method above which ignores the corner effect.

In order to investigate the stress intensity factor for the whole propagation event of the kinked crack, the normalized time t_f/t is chosen as the parameter. The instant of initiation of the kink is at $t_f/t = 1$, while $t_f/t = 0$ corresponds to the time when the kinked crack has propagated for an infinite time compared to the delay time. We choose two kinking angles $\delta = \pi/8$, $\pi/4$ and plot the non-dimensional stress intensity factor for mode I and mode II vs t_f/t for incident normal stress wave loading. The results are shown in Figs 5 and 6. The mode I stress intensity factor is almost constant which shows that K_I^L weakly depends on the delay time t_f. From the result shown in eqn (2.12) (from Ref. [3]), K_I^L is independent of the delay time for stress wave loading when $\delta = 0$. We would expect that for small kink angles this also holds. Hence, the simple expression of the mode I stress intensity factor shown in eqn (29) can be used to calculate K_I^L for the whole propagation history of a small kinked angle for any kinked angle for a short time period after the crack is kinked. The mode II stress intensity factor has a stronger dependence on delay time as shown in Fig. 6. Note that the results for $\delta = 0$ are available in Ref. [3].

The corresponding energy flux into the kinked crack is plotted in Fig. 7. If the maximum energy release rate criterion is accepted as the kinking condition, then the combination of the kinking angle and the crack speed can be determined at which the energy flux into the

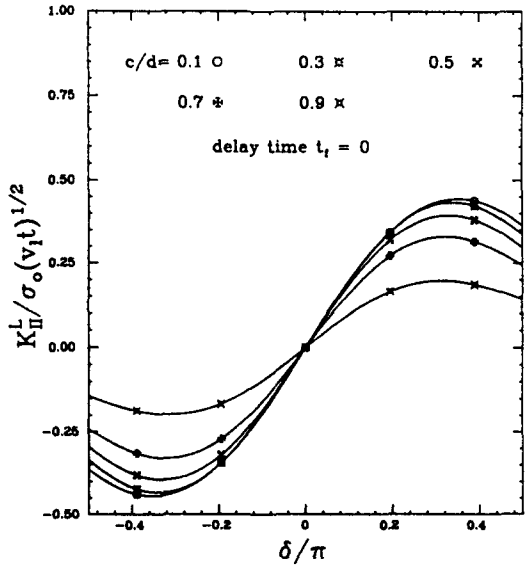

Fig. 4.The normalized mode II stress intensity factor vs kinking angle for $t_f = 0$ for different values of crack speed due to incident longitudinal stress wave loading.

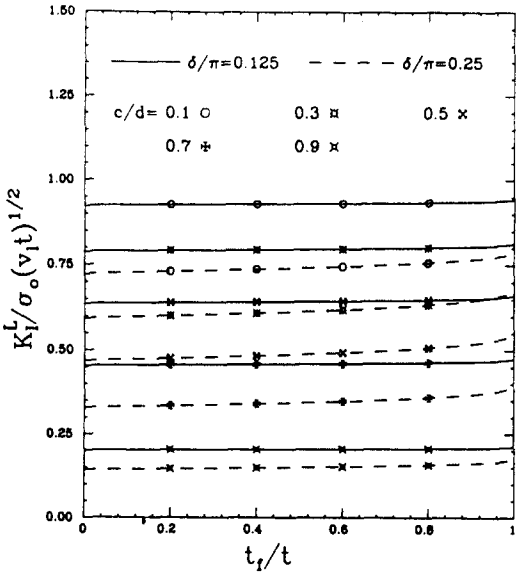

Fig. 5. The time history of the mode I stress intensity factor for $\delta = \pi/8, \pi/4$ for different values of crack speed due to incident longitudinal stress wave loading.

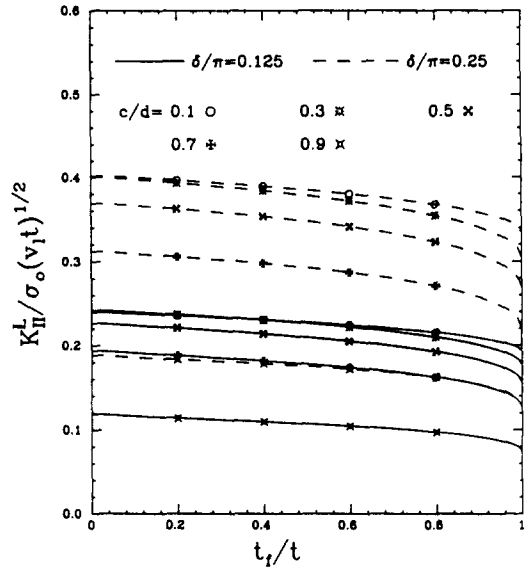

Fig. 6. The time history of the mode II stress intensity factor for $\delta = \pi/8, \pi/4$ for different values of crack speed due to incident longitudinal stress wave loading.

propagating crack tip achieves a maximum value. For the stress wave loading case, the crack will tend to propagate straight ahead of the original crack with a constant crack speed $v_c = 0.56v_r$ which makes $E^*_{max} = 0.358$ for the whole propagating time.

The other loading condition that is also of interest is to apply uniform normal loading on the original crack faces. The mode I and II stress intensity factors can be obtained from eqns (25) and (30) as shown in Figs 8 and 9. For this loading case, the stress intensity factor depends strongly on the delay time. If we neglect the delay time effect as in Ref. [14], we always underestimate both mode I and mode II stress intensity factors especially in the time period when kinking has just occurred. The energy flux into the crack tip is shown in Fig. 10. If the maximum energy release rate criterion is applied for this case, the new crack would again tend to propagate out along the original crack line. The value of E^*_{max} and the corresponding crack velocity are plotted as a function of t_f/t in Fig. 11. This result also indicates that for the crack face loading case, the crack would most likely slow down during the propagation event. The theoretical prediction for a crack propagating straight ahead is also observed experimentally[5–8] for crack face loading and for stress wave loading[20].

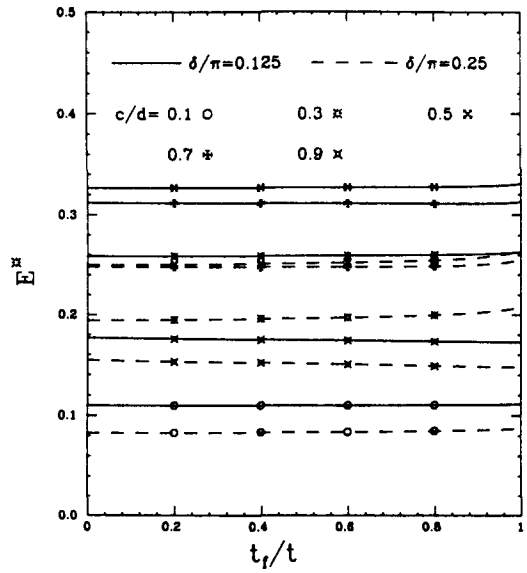

Fig. 7. The corresponding energy flux into the kinking crack tip for Figs 5 and 6.

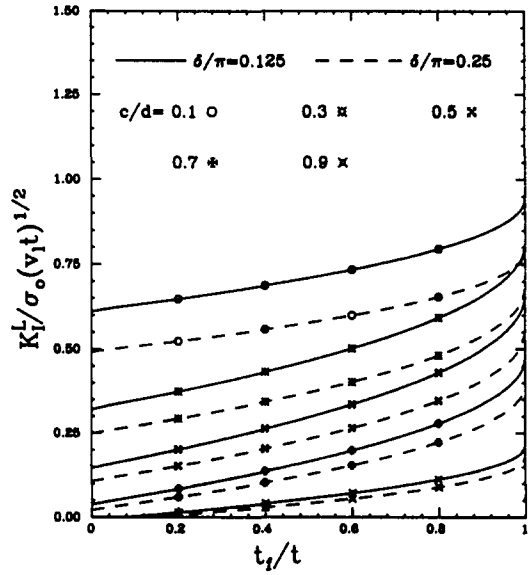

Fig. 8. The time history of the mode I stress intensity factor for $\delta = \pi/8, \pi/4$ for different values of crack speed due to a normal uniform stress applied to the original crack faces.

MIXED MODE CRACK KINKING DUE TO AN INCIDENT TRANSVERSE WAVE

The incident stress wave is a vertically polarized transverse wave of the form

$$\sigma^{i}_{xz} = \sigma_0 H(tv_s - z). \tag{35}$$

The stress components in the polar coordinate for incident and diffracted fields of the stationary crack are

$$\sigma^{i}_{\theta\theta} = -\sigma_0 \sin 2\theta \tag{36a}$$

$$\sigma^{i}_{\theta r} = \sigma_0 \cos 2\theta \tag{36b}$$

$$\sigma^{d}_{\theta\theta} = \frac{1}{2}(1-\cos 2\theta)\sigma^{II}_{xx} + \frac{1}{2}(1+\cos 2\theta)\sigma^{II}_{zz} - \sin 2\theta\, \sigma^{II}_{xz} \tag{37a}$$

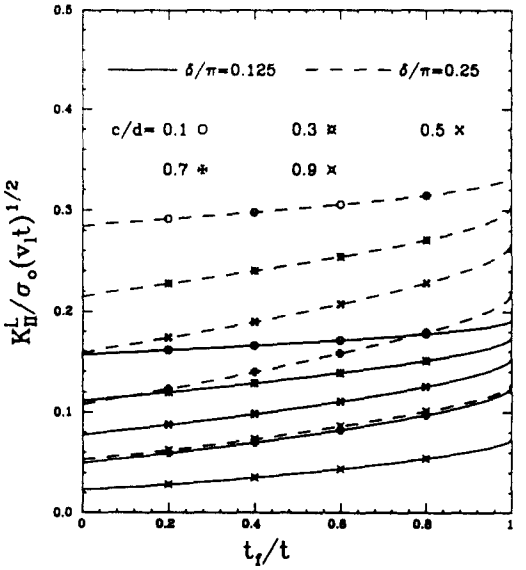

Fig. 9. The time history of the mode II stress intensity factor for $\delta = \pi/8, \pi/4$ for different values of crack speed due to a normal uniform stress applied to the original crack faces.

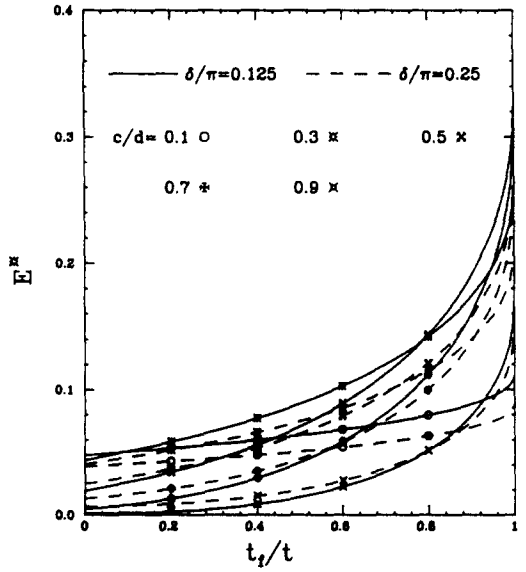

Fig. 10. The corresponding energy flux into the kinking crack tip for Figs 8 and 9.

$$\sigma_{0r}^{d} = -\frac{1}{2}\sin 2\theta\,\sigma_{xx}^{II} + \frac{1}{2}\sin 2\theta\,\sigma_{zz}^{II} + \cos 2\theta\,\sigma_{xz}^{II} \tag{37b}$$

where σ_{xx}^{II}, σ_{xz}^{II} and σ_{zz}^{II} are expressed in eqns (9a)–(9c). For the approximate method, the conditions on the crack faces are the same as shown in eqns (21) and (22) for calculating mode I and II stress intensity factors. The analysis for the stress intensity factor due to an incident vertically polarized transverse wave on a kinked crack proceeds in a very similar manner as discussed in the previous section for the longitudinal wave. We will not repeat the solution procedure here.

The mode I stress intensity factor is

$$K_I^T = (K_I^T)_d + (K_I^T)_i \tag{38}$$

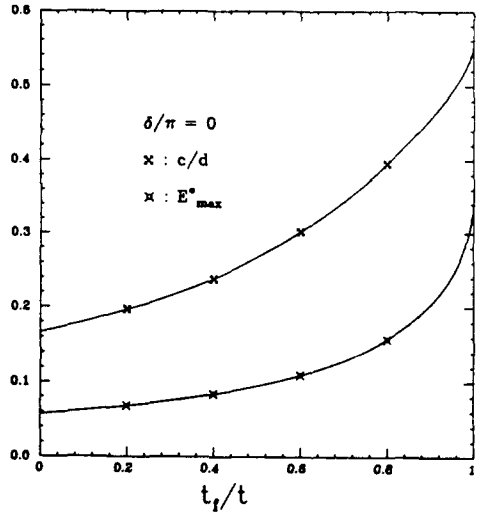

Fig. 11. Kinking angle and crack tip speeds which make E^* maximum during the propagating event by applying normal uniform stress on the original crack faces.

$$(K_I^T)_d(t, v_c, \delta) = 2\sigma_0\left[\frac{2t_f}{\pi d(1-a/d)}\right]^{1/2}\left\{w_+(d)(d^*-d)^{1/2}\sin 2\delta - \frac{3u_0 d w_+(d)}{4}\left(\sin\frac{\delta}{2}+\sin\frac{3\delta}{2}\right) - \frac{u_0 d}{\pi}\int_{d+\varepsilon}^{d^*}\frac{(d^*-h)^{1/2}}{(h-d)^{1/2}} \times\left[\frac{3w_+(d)}{4(h-d)}\left(\sin\frac{\delta}{2}+\sin\frac{3\delta}{2}\right) - \frac{w_+(h)d^{5/2}}{k(h-d)^3}(\sigma_{\theta\theta}^T)_h^*\right]dh\right\} + o(1) \quad (39)$$

$$(K_I^T)_i(t, v_c, \delta) = \frac{2\sqrt{2}\,\sigma_0 t_f^{1/2} w_+(d)(d^*-d)^{1/2}}{\sqrt{\pi}(1-a/d)^{1/2}d^{1/2}}\sin 2\delta \quad (40)$$

and

$$K_I^T = -\frac{3}{2}\sqrt{\left(\frac{2}{\pi}\right)}\sigma_0 u_0 \kappa(d) t^{1/2}\left(\sin\frac{\delta}{2}+\sin\frac{3\delta}{2}\right) = -\frac{3}{4}K_I^3\kappa(d)\left(\sin\frac{\delta}{2}+\sin\frac{3\delta}{2}\right) \quad \text{as } t\to t_f. \quad (41)$$

The mode II stress intensity factor is

$$K_{II}^T = (K_{II}^T)_d + (K_{II}^T)_i \quad (42)$$

$$(K_{II}^T)_d(t, v_c, \delta) = 2\sigma_0\left[\frac{2t_f}{\pi d(1-b/d)}\right]^{1/2}\left\{-u_+(d)(d^*-d)^{1/2}\cos 2\delta + \frac{u_0 d u_+(d)}{4}\left(\cos\frac{\delta}{2}+3\cos\frac{3\delta}{2}\right) + \frac{u_0 d}{\pi}\int_d^{d^*}\frac{(d^*-h)^{1/2}}{(h-d)^{1/2}}\left[\frac{u_+(d)}{4(h-d)} \times\left(\cos\frac{\delta}{2}+3\cos\frac{3\delta}{2}\right) - \frac{u_+(h)d^{5/2}}{k(h-d)^3}(\sigma_{\theta r}^T)_h^*\right]dh\right\} + o(1) \quad (43)$$

$$(K_{II}^T)_i(t, v_c, \delta) = \frac{2\sqrt{2}\,\sigma_0 t_f^{1/2} u_+(d)(d^*-d)^{1/2}}{\sqrt{\pi}(1-b/d)^{1/2}d^{1/2}}\cos 2\delta \quad (44)$$

and

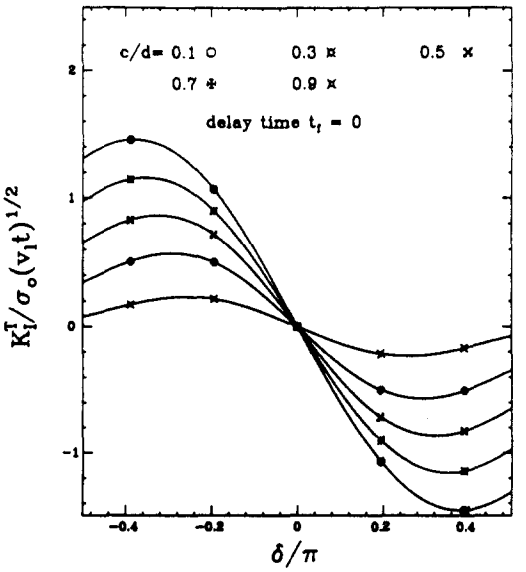

Fig. 12. The normalized mode I stress intensity factor vs kinking angle for $t_F = 0$ for different values of crack speed due to incident transverse stress wave loading.

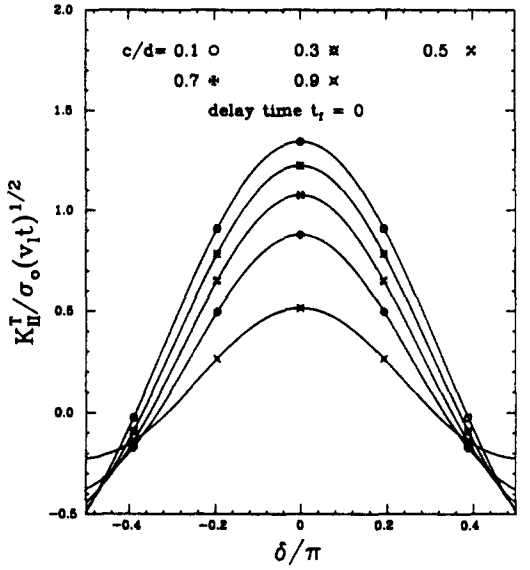

Fig. 13. The normalized mode II stress intensity factor vs kinking angle for $t_f = 0$ for different values of crack speed due to incident transverse stress wave loading.

$$K_{II}^T = \frac{\sqrt{2}\,\sigma_0 u_0 u_+(d)\,(dt)^{1/2}}{2\sqrt{\pi}\,(1-b/d)^{1/2}}\left(\cos\frac{\delta}{2} + 3\cos\frac{3\delta}{2}\right) \quad \text{as } t \to t_f. \tag{45}$$

Both $(\sigma_{\theta\theta}^T)_h^*$ and $(\sigma_{\theta r}^T)_h^*$ are given in Appendix B. The numerical results of the mode I and II stress intensity factors for $t_f = 0$ are shown in Figs 12 and 13, respectively. The mode I results again show a similar accuracy as for an incident longitudinal wave if compared to Ref. [12]. Reference [14] also obtains the same results for the mode I stress intensity factor. For mode II, the accuracy is not so good as in the longitudinal stress wave case, especially for lower crack tip speeds and high kinking angles, but it is in better agreement with Ref. [12] than Ref. [14].

The stress intensity factors including the delay time effect for kinking angle $\delta = \pi/8$ and $\pi/4$ are plotted in Figs 14 and 15. The results again show the weak dependence on the delay time for small kink angles for an incident transverse stress wave. The corresponding energy flux into the kinked crack tip is shown in Fig. 16. Using a maximum energy release

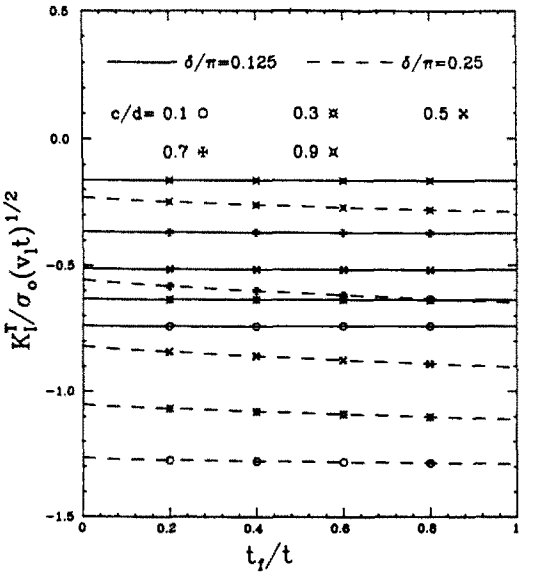

Fig. 14. The time history of the mode I stress intensity factor for $\delta = \pi/8, \pi/4$ for different values of crack speed due to incident transverse stress wave loading.

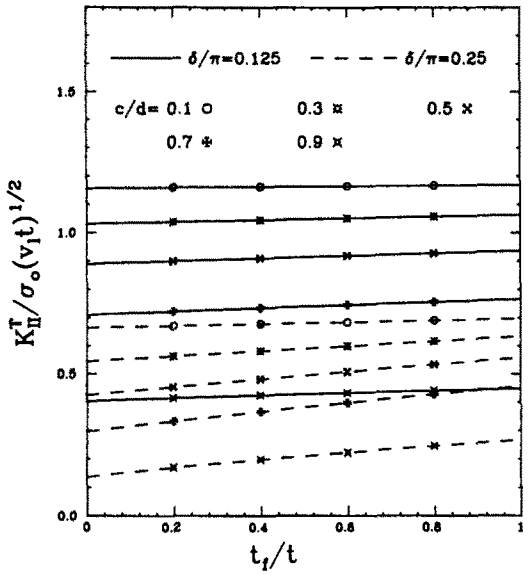

Fig. 15. The time history of the mode II stress intensity factor for $\delta = \pi/8, \pi/4$ for different values of crack speed due to incident transverse stress wave loading.

rate criterion, the new crack would again tend to propagate straight out of the original crack with a constant speed $v_c = 0.675v_r$, which gives $E^*_{max} = 0.84$.

DISCUSSION

In this paper, a delay time is included before the initiation of the new kinking crack. This makes the model a great deal more realistic physically. An approximate method that ignores the corner geometry of the kink angle is used to construct the mixed mode stress intensity factor. A very satisfactory result is obtained when compared with the numerical results[12] with no delay time effect. It is also shown that the stress intensity factor immediately after kinking can be expressed in the form of a universal function of the crack tip speed times the stress intensity factor appropriate for the given diffraction process with no crack-tip motion times a spatial angular dependence which is independent of crack tip velocity or loading. It is unfortunately not yet clear from experimental results what is a suitable criterion for a bifurcation event. With these theoretical results for the stress intensity

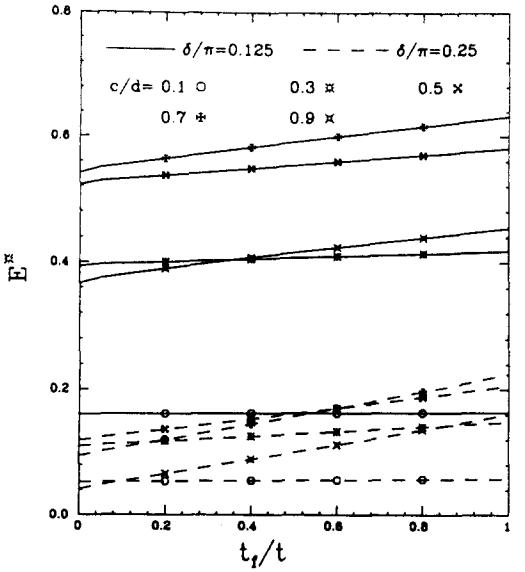

Fig. 16. The corresponding energy flux into the kinking crack tip for Figs 14 and 15.

factor at hand, an attempt can be made to determine the kink angle and the new kinked crack speed using different fracture criteria and to compare them with the experimental results available. For this paper, the maximum energy release rate is adopted for the kinking criterion, for both the incident stress wave case or applied loading on the original crack faces case. In either situation, the crack will tend to remain straight.

The complete solutions available for the kinked crack geometry that include the corner effect are still restricted to no delay time; see Ref. [11] for the theoretical results of the anti-plane mode and Refs [12, 13] for numerical results of the in-plane mode. There are no other results that can be used to judge the accuracy of the approximation in this paper when the delay time effect is included in the whole kinking angle range. It has been shown, that for $\delta = 0$, the results of this paper can reduce to the exact solution in Ref. [3] which also includes the delay time effect. It is believed that this approximate method still gives quite good accuracy for small kinked angles. The accuracy of the results presented in this paper for the stress intensity factor at high kink angles including finite delay time still needs to be checked by other numerical results, but would also appear to be quite good.

It has been observed in experiments[5–8, 20] for both applied loading on the original crack faces and incident stress wave loading that the crack will most likely grow straight ahead of the original crack for some time and then bifurcate or kink. This problem is much more difficult to solve. The complete stress fields of a suddenly stopping crack must first be worked out. The stresses along the kinked crack line must then be cancelled by a kinking crack problem. A similar method to the one used in this paper may then be applied. The details of these calculations for mode III will appear shortly.

Acknowledgements—The authors would like to thank Professor L. B. Freund for helpful discussions. The support of the authors by the National Science Foundation, Solid Mechanics Program through Grant MEA-8306644 is gratefully acknowledged. The calculations were performed in the VAX-11/780 Computational Mechanics Facility at Brown University. This facility was made possible by grants from the National Science Foundation (Solid Mechanics Program), the General Electric Foundation, and the Digital Equipment Corporation.

REFERENCES

1. L. B. Freund, Crack propagation in an elastic solid subjected to general loading—I. Constant rate of extension. *J. Mech. Phys. Solids* **20**, 129–140 (1972).
2. L. B. Freund, Crack propagation in an elastic solid subjected to general loading—II. Non-uniform rate of extension. *J. Mech. Phys. Solids* **20**, 141–152 (1972).
3. L. B. Freund, Crack propagation in an elastic solid subjected to general loading—III. Stress wave loadings. *J. Mech. Phys. Solids* **21**, 47–61 (1973).
4. L. B. Freund, Crack propagation in an elastic solid subjected to general loading—IV. Obliquely incident stress pulse. *J. Mech. Phys. Solids* **22**, 137–146 (1974).

5. K. Ravi-Chandar and W. G. Knauss, An experimental investigation into dynamic fracture: I. Crack initiation and arrest. *Int. J. Fracture* **25**, 247 262 (1984).
6. K. Ravi-Chandar and W. G. Knauss, An experimental investigation into dynamic fracture: II. Microstructural aspects. *Int. J. Fracture* **26**, 65–80 (1984).
7. K. Ravi-Chandar and W. G. Knauss, An experimental investigation into dynamic fracture: III. On steady-state crack propagation and crack branching. *Int. J. Fracture* **26**, 141–154 (1984).
8. K. Ravi-Chandar and W. G. Knauss, An experimental investigation into dynamic fracture: IV. On the interaction of stress waves with propagating cracks. *Int. J. Fracture* **26**, 189–200 (1984).
9. P. Burgers and J. P. Dempsey, Two analytical solutions for dynamic crack bifurcation in anti-plane strain. *J. Appl. Mech.* **49**, 366 370 (1982).
10. P. Burgers, Dynamic propagation of a kinked or bifurcated crack in anti-plane strain. *J. Appl. Mech.* **49**, 371–376 (1982).
11. J. P. Dempsey, M. K. Kuo and J. D. Achenbach, Mode III crack kinking under stress wave loading. *Wave Motion* **4**, 181–190 (1982).
12. P. Burgers, Dynamic kinking of a crack in plane strain. *Int. J. Solids Structures* **19**, 735–752 (1983).
13. P. Burgers and J. P. Dempsey, Plane strain dynamic crack bifurcation. *Int. J. Solids Structures* **20**, 609–618 (1984).
14. J. D. Achenbach, M. K. Kuo and J. P. Dempsey, Mode III and mixed mode I–II crack kinking under stress-wave loading. *Int. J. Solids Structures* **20**, 395–410 (1984).
15. C. C. Ma and P. Burgers, Mode III crack kinking with delay time. An analytical approximation, *Int. J. Solids Structures* **22**, 883–899 (1986).
16. M. K. Kuo and J. D. Achenbach, Conditions for crack kinking under stress-wave loading. *Int. J. Solids Structures* (1987), in press.
17. A. T. De Hoop, Representation theorems for the displacement in an elastic solid and their application to elastodynamic diffraction theory, Doctoral Dissertation, Technische Hogeschool, Delft (1958).
18. A. F. Fossum and L. B. Freund, Nonuniformly moving shear crack model of a shallow force earthquake and mechanism. *J. Geophys. Res.* **80**, 3343–3347 (1975).
19. L. B. Freund and R. J. Clifton, On the uniqueness of elastodynamic solutions of running cracks. *J. Elasticity* **4**, 293–299 (1974).
20. G. Ravi-Chandran, Dynamic fracture under plane wave loading, Ph.D. Thesis, Brown University (1986).

APPENDIX A

$$(\sigma^L_{\theta\theta})^*_h = \frac{1}{2}(1-\cos 2\delta)\,(\sigma^L_{xx})^*_h + \frac{1}{2}(1+\cos 2\delta)\,(\sigma^L_{zz})^*_h - \sin 2\delta\,(\sigma^L_{xz})^*_h$$

$$(\sigma^L_{\theta r})^*_h = -\frac{1}{2}\sin 2\delta\,(\sigma^L_{xx})^*_h + \frac{1}{2}\sin 2\delta\,(\sigma^L_{zz})^*_h + \cos 2\delta\,(\sigma^L_{xz})^*_h$$

and

$$(\sigma^L_{zz})^*_h = \operatorname{Im}\left\{-\frac{[2\Theta_a^2+b^2(v_c h-1)^2]^2\Omega_a}{\Psi_a\Theta_a[a(v_c h-1)+\Theta_a]^{1/2}} - \frac{4\Theta_b[a(v_c h-1)-\Theta_b]^{1/2}[b^2(v_c h-1)^2-\Theta_b^2]^{1/2}\Omega_b}{\Psi_b}\right\}$$

$$(\sigma^L_{xz})^*_h = \operatorname{Im}\left\{-\frac{2[a(v_c h-1)-\Theta_a]^{1/2}[2\Theta_a^2-b^2(v_c h-1)^2\Omega_a}{\Psi_a} + \frac{2[a(v_c h-1)+\Theta_b]^{1/2}[2\Theta_b^2-b^2(v_c h-1)^2]\Omega_b}{\Psi_b}\right\}$$

$$(\sigma^L_{xx})^*_h = \operatorname{Im}\left\{\frac{[2\Theta_a^2-b^2(v_c h-1)^2][2\Theta_a^2+(b^2-2a^2)(v_c h-1)^2]\Omega_a}{\Psi_a\Theta_a[a(v_c h-1)+\Theta_a]^{1/2}} + \frac{4\Theta_b[a(v_c h-1)-\Theta_b]^{1/2}[b^2(v_c h-1)^2-\Theta_b^2]^{1/2}\Omega_b}{\Psi_b}\right\}$$

where

$$\Omega_a = -[h^2-a^2(vh-1)^2]^{1/2}\cos\delta + ih\sin\delta$$

$$\Omega_b = -[h-b^2(vh-1)^2]^{1/2}\cos\delta + ih\sin\delta$$

$$\Theta_a = -h\cos\delta + i[h^2-a^2(vh-1)^2]^{1/2}\sin\delta$$

$$\Theta_b = -h\cos\delta + i[h^2-b^2(vh-1)^2]^{1/2}\sin\delta$$

$$\Psi_a = [h^2-a^2(vh-1)^2]^{1/2}[\Theta_a - c(vh-1)]S^0_-(\Theta_a/(vh-1))$$

$$\Psi_b = [h^2-b^2(vh-1)^2]^{1/2}[\Theta_b - c(vh-1)]S^0_-(\Theta_b/(vh-1)).$$

APPENDIX B

$$(\sigma_{\theta\theta}^T)_h^* = \frac{1}{2}(1-\cos 2\delta)(\sigma_{xx}^T)_h^* + \frac{1}{2}(1+\cos 2\delta)(\sigma_{zz}^T)_h^* - \sin 2\delta\ (\sigma_{xz}^T)_h^*$$

$$(\sigma_{\theta r}^T)_h^* = -\frac{1}{2}\sin 2\delta\ (\sigma_{xx}^T)_h^* + \frac{1}{2}\sin 2\delta\ (\sigma_{zz}^T)_h^* + \cos 2\delta\ (\sigma_{xz}^T)_h^*$$

and

$$(\sigma_{zz}^T)_h^* = \mathrm{Im}\left\{\frac{2[b(v_c h-1)-\Theta_a]^{1/2}[b^2(v_c h-1)^2-2\Theta_a^2]\Omega_a}{\Psi_a} - \frac{2[b(v_c h-1)-\Theta_b]^{1/2}[b^2(v_c h-1)^2-2\Theta_b^2]\Omega_b}{\Psi_b}\right\}$$

$$(\sigma_{xz}^T)_h^* = \mathrm{Im}\left\{\frac{4\Theta_a[b(v_c h-1)-\Theta_a]^{1/2}[a^2(v_c h-1)^2-\Theta_a^2]^{1/2}\Omega_a}{\Psi_a} - \frac{[2\Theta_b^2-b^2(v_c h-1)^2]^2\Omega_b}{\Psi_b\Theta_b[b(v_c h-1)+\Theta_b]^{1/2}}\right\}$$

$$(\sigma_{xx}^T)_h^* = \mathrm{Im}\left\{\frac{2[b(v_c h-1)-\Theta_a]^{1/2}[2\Theta_a^2+(b^2-2a^2)(v_c h-1)^2]\Omega_a}{\Psi_a} + \frac{2[b(v_c h-1)+\Theta_b]^{1/2}[b^2(v_c h-1)^2-2\Theta_b^2]\Omega_b}{\Psi_b}\right\}.$$